Asymmetric apportioning of aged mitochondria between daughter cells is required for stemness

Pekka Katajisto[1,2,3,#], **Julia Döhla**[3], **Christine Chaffer**[1], **Nalle Pentinmikko**[3], **Nemanja Marjanovic**[1], **Sharif Iqbal**[3], **Roberto Zoncu**[1,2], **Walter Chen**[1,2], **Robert A. Weinberg**[1], and **David M. Sabatini**[1,2,#]

[1]Whitehead Institute for Biomedical Research, Boston, MA 02142 USA; Department of Biology, MIT, Cambridge, MA 02139, USA [2]Howard Hughes Medical Institute, MIT, Cambridge, MA 02139, USA [3]Institute of Biotechnology, University of Helsinki, P.O. box 00014, Helsinki, Finland

Abstract

By dividing asymmetrically, stem cells can generate two daughter cells with distinct fates. However, evidence is limited in mammalian systems for the selective apportioning of subcellular contents between daughters. We followed the fates of old and young organelles during the division of human mammary stem-like cells and found that such cells apportion aged mitochondria asymmetrically between daughter cells. Daughter cells that received fewer old mitochondria maintained stem cell traits. Inhibition of mitochondrial fission disrupted both the age-dependent sub-cellular localization and segregation of mitochondria, and caused loss of stem cell properties in the progeny cells. Hence, mechanisms exist for mammalian stem-like cells to asymmetrically sort aged and young mitochondria, and these are important for maintaining stemness properties.

Stem cells can divide asymmetrically to generate a new stem cell and a progenitor cell that gives rise to the differentiated cells of a tissue. During organismal aging it is likely that stem cells sustain cumulative damage, which may lead to stem cell exhaustion and eventually compromise tissue function (1). To slow the accumulation of such damage, stem cells might segregate damaged subcellular components away from the daughter cell destined to become a new stem cell. Although non-mammalian organisms can apportion certain non-nuclear cellular compartments (2–4) and oxidatively damaged proteins (5, 6) asymmetrically during cell division, it is unclear whether mammalian stem cells can do so as well (6–9).

We used stem-like cells (SLCs) recently identified in cultures of immortalized human mammary epithelial cells (10) to test whether mammalian stem cells can differentially apportion aged, potentially damaged, subcellular components, such as organelles between daughter cells. These SLCs express genes associated with stemness, form mammospheres, and, after transformation, can initiate tumors in vivo (10, 11). Moreover, because of their round morphology, the SLCs can be distinguished by visual inspection from the flat, tightly adherent, non-stem-like mammary epithelial cells with which they coexist in monolayer cultures (Fig. 1B).

[#]Address correspondence to: pekka.katajisto@helsinki.fi or sabatini@wi.mit.edu.

To monitor the fate of aged subcellular components, we expressed photoactivatable green fluorescent protein (paGFP) (12) in lysosomes, mitochondria, the Golgi, ribosomes, and chromatin, by fusing the fluorescent protein to the appropriate targeting signals or proteins (Supplementary table 1). paGFP fluoresces only after exposure to a pulse of UV-light (12), allowing us to label each component in a temporally controlled fashion (Fig. 1A). Because synthesis of paGFP continues after the light pulse, cells subsequently accumulate unlabeled 'young' components in addition to the labeled 'old' components; these can be either segregated in distinct subcellular compartments or commingled within individual cells.

We followed the behavior of labeled components in single round SLCs or flat epithelial cells and focused on cell divisions that occurred 10 to 20 hours after paGFP photoactivation (Fig. 1B). The epithelial cells symmetrically apportioned all cellular components analyzed (Fig. 1B). In contrast, the round SLCs apportioned ~5.6-fold more (p<0.001, t-test) of   10 hour-old mitochondrial outer membrane protein 25 (paGFP-Omp25) to one daughter cell than the other (Fig. 1B). Similarly labeled markers for all other organelles examined were apportioned symmetrically. We designated the daughter cell that inherited more aged Omp25 from the mother cell as Progeny1 (P1) and the other as Progeny2 (P2).

To test whether the same cells that asymmetrically apportion the mitochondrial membrane protein also allocate other membrane compartments asymmetrically, we labeled SLCs with the lipophilic dye PKH26 before photoactivation of paGFP-Omp25. PKH26 initially labels the plasma membrane and is gradually endocytosed to form distinct cytoplasmic puncta and it is relatively symmetrically apportioned during division of hematopoietic cells (13). SLCs apportioned old mitochondria asymmetrically, but the same cells apportioned PKH26 symmetrically (Fig. 1C, Supplementary movie 1). In contrast, the epithelial cells apportioned both paGFP-Omp25 and PKH26 symmetrically (Fig. 1C, Supplementary movie 2), similarly to mouse embryonic fibroblasts (data not shown).

To verify that SLCs indeed apportion mitochondria according to the age of the organelle, we analyzed the apportioning of paGFP-Omp25 in cell divisions that occurred at random times after the initial photoactivation. We assumed that the age of Omp25 molecules reflected the age of the mitochondria with which they were associated. Cells that divided 0–10 hours after photoactivation showed symmetric apportioning of paGFP-Omp25 (Fig. 1D). However, cells that divided more than 10 hours after photoactivation and thus carried fluorescent marks only on organelles that were at least 10 hours old, apportioned their labeled mitochondria asymmetrically (Fig. 1D).

To follow the apportioning of two different age-classes of mitochondria, we tagged mitochondria with mitochondrial proteins fused to a Snap-tag (14). Snap-tag is a derivatized DNA repair enzyme, O^6-alkylguanine-DNA alkyltransferase, which can covalently link various fluorophores to the tagged fusion protein in live cells. We used two Snap-tag substrates with two different fluorophores (red and green) sequentially to separately label young and old organelles (Fig. 2A). Snap-tags are rendered inactive by the labeling reaction; this ensures that the two colors will mark chronologically distinct populations, and, in contrast to previously used strategies (15), allows precise timing of labeling. Moreover,

Snap-tags allow uniform labeling throughout the entire cell and the simultaneous labeling of multiple cells, and avoid the risk of phototoxic artifacts associated with paGFP (16).

We analyzed divisions of SLCs expressing Snap-Omp25 and carrying red and green fluorophores on what we refer to as old and young mitochondria, labeled 48 to 58 and 0 to 10 hours before division, respectively (Fig. 2B, Supplementary movie 3). After cell division, the old label from the mother cell was divided more asymmetrically between daughter cells than the young label (old: P1 89% vs P2 11% of the mother cell intensity, p=0.004; young: 67% vs 33%, p=0.04, n=5). (Fig. 2B,C; Fig. S1). This age-specific apportioning reduced the relative portion of old mitochondria in P2 to about one fifth of those in the mother cell and one sixth of those in the P1 daughter (Fig. S2A). However, cells that inherited fewer old mitochondria contained similar total amounts of mitochondria (Fig. S3), suggesting that unlabeled new mitochondria generated after the 'young labeling' were differentially distributed to balance the overall mitochondrial quantity between the two daughters. We also targeted the mitochondrial inner membrane (see Fig. S4 for mitochondrial constructs used) by expressing COX8A-Snap in SLCs. This inner membrane protein showed asymmetric distribution comparable to that of Omp25 (Fig. 2C), increasing our confidence that the age-selective segregation of Omp25 represented that of whole mitochondria.

Our analyses of asymmetric cell divisions indicated that the majority of mitochondria in the stem-like mother cells contained both old and young labels, whereas some mitochondria carried only young or old label (Fig. 2B). Most mitochondria carrying exclusively young label apportioned to the P2 daughter cells, whereas mitochondria containing a mix of the two labels segregated to P1 cells (Fig. 2B). Moreover, the small quantity of old label received by P2 did not co-localize with young label (Fig. 2B, S2B). These findings indicate that even before cell division, the stem-like mother cell keeps new mitochondria apart from old ones, and passes these younger mitochondria preferentially to the P2 daughter.

To study such segregation in greater detail, we analyzed SLCs immediately after labeling of the young mitochondria but before division (Fig. S5, Fig. 2D). Old mitochondria tended to localize perinuclearly and in some cells formed puncta containing exclusively old label (Fig. S5, S6), whereas the young label distributed throughout the mitochondrial network more evenly. To address if such localization differences could contribute to the demonstrated age-specific apportioning, we imaged old and young mitochondria with live-microscopy within the 10-hour window we used for analyses of asymmetric division (Fig. 2E). Young (green) label gradually became more perinuclear as it became older, but at 10 hours after labeling, which was the maximum time point used for the quantitation of asymmetry in cell division, there was still a significant difference in the localization of the two labels (Fig. 2E). The perinuclear localization of old label did not occur in a fibroblast cell line without stem-like properties (Fig. S6), and it did not result from old label entering and marking other subcellular components, such as lysosomes, due to mitochondrial turnover (Fig. S7). However, within the interconnected mitochondrial network, we identified specific domains that were enriched for old label (Fig. 2D). These data support the notion that mother SLCs localize new and old mitochondria to specific cytoplasmic regions, ostensibly to facilitate the exclusion of old mitochondria from future P2 daughter cells.

The asymmetric apportioning and localization of mitochondria in the daughter cells suggested that daughter cells resulting from a division of a SLC might represent the founders of two lineages, one stem-like and the other more likely to differentiate. We used flow cytometry to analyze the age-selective apportioning of mitochondria in cell populations that had been synchronized to divide in concert (Fig. S8, Fig. 3A). Some divided cells received significantly fewer older mitochondria than did others, whereas the young mitochondria were more uniformly distributed. Upon FACS-sorting and re-plating of daughter cell populations, the Pop1 cells, which received more old mitochondria, were morphologically flatter and more adherent than the Pop2 cells (Fig. 3A). Three days after cell sorting, the Pop1 cells formed clusters with a monolayer appearance, whereas the Pop2 cells regenerated both round and flat cells similar to the original parental population. However, both populations had similar rates of proliferation (Fig. S9). Thus Pop2 cells, which received fewer older mitochondria, appeared to represent the SLCs that could subsequently undergo asymmetric divisions.

We used the ability to form mammospheres in 3-dimensional culture as an *in vitro* assay of mammary epithelial cell stemness (17). In this assay the Pop2 of both Snap-Omp25 and COX8a-Snap expressing cells formed 3 times more mammospheres per 1000 cells than Pop1 (Fig. 3B). Hence, the cells that inherited fewer old mitochondria during an asymmetric division were, by the criterion of mammosphere-forming ability, more stem-like.

Mitochondria that have lower membrane potential (Ψm)–an index of mitochondrial function– localize perinuclearly (18), and high Ψm is linked to stem-like traits (19, 20). Moreover, in *S. cerevisiae* the Ψm-driven selective inheritance of fit mitochondria is required for the daughter cell to maintain full replicative lifespan (21, 22). We analyzed the Ψm of cells in the Pop1 and Pop2 populations to address whether their mitochondria differ functionally. As the results with two different Ψm indicator dyes were not consistent (Fig. S10), we analyzed the age-selective apportioning of mitochondria in the presence of a mitochondrial uncoupler, carbonyl cyanide *m*-chlorophenyl hydrazone (CCCP). Alterations of the Ψm had no effect on the age-selective segregation of mitochondria in an SLC division (Fig. S11, S12). However, we did note a significant correlation between mammosphere-forming capacity and Ψm with both dyes (Fig. S10). Thus, we conclude that although Ψm correlates with stem-like properties, it is not the signal that guides the age-selective asymmetric segregation of mitochondria during mammalian cell division.

Cells have mitochondrial quality control mechanisms through which they specifically remove poorly functional parts of their mitochondrial network. Following mitochondrial fission, which depends on the dynamin-related protein 1 (Drp1) (23), the kinase PINK1 will promote the recruitment of the Parkin E3 ubiquitin ligase to mitochondrial fragments with low Ψm and induce their selective autophagy (24). Another PINK1/Parkin-dependent (but Ψm- and Drp1-independent) mitochondrial quality control mechanism is mediated by generation of Mitochondrially Derived Vesicles (MDVs) that target oxidatively damaged mitochondrial components for lysosomal degradation (25).

SLCs and epithelial cells had comparable numbers of autophagosomes containing old mitochondrial label (Fig. S13) indicating that degradation via the autophagosome-lysosome

pathway is not directly responsible for the reduction in the numbers of old mitochondria in stem-like cells. However, SLCs had a higher mitophagy/autophagy-ratio (Fig. S13E), suggesting that high quality of mitochondria may be relevant for the SLC state and asymmetric apportioning during cell division. To test this, we transfected synchronized cells with siRNAs targeting Parkin, or treated cells with the Drp1 inhibitor mDivi-1 (26) to inhibit mitochondrial fission. In both cases, we observed a significant and similar reduction in the number of cells inheriting mostly young mitochondria (Pop2) and a concomitant increase in cells inheriting a mixture of old and young mitochondria (Pop1) (Fig. 4A, S14). Surprisingly, fragmentation of mitochondria by Drp1 expression resulted in comparable reduction in the Pop2 with mDivi-1 or siParkin (Fig. S15). However, these effects are probably not caused by the changes of the mitochondrial network status, as round SLCs and differentiated cells have similar mitochondrial network connectivity (Fig. S16, supplementary movie 5). Taken together, these data suggest that any perturbation that challenges normal mitochondrial quality control mechanisms will either serve as a signal for an SLC to stop asymmetric segregation of mitochondria, or alternatively, overload the capacity of the SLCs to effectively apportion old mitochondria asymmetrically.

To address whether the preferential acquisition of younger mitochondria contributed to maintenance of stem cell function, we analyzed the mammosphere-forming capacity of the cells remaining in Pop2 after a division in the presence of either siParkin or mDivi-1. Both treatments eliminated the increased stemness capacity of the remaining Pop2 cells so that they formed mammospheres with the lower efficiency characteristic of the Pop1 cells (Fig. 4B). However, the cells in Pop2 from mDivi-1-treated samples proliferated similarly to controltreated cells in 2D-culture (Fig. S14B). Moreover, because the analysis of mammosphere formation was conducted in the absence of mDivi-1, these data suggest that the failure to asymmetrically apportion old mitochondria in a single division caused a persistent loss of stemness in SLCs.

To understand how alterations of mitochondrial dynamics and quality control might eliminate the age-selective apportioning, we administered mDivi-1 to cells 46 hours after labeling old mitochondria and followed the cells with live-microscopy. The old mitochondrial label that had been confined to the perinuclear region spread throughout the mitochondrial network of the cell periphery after mDivi-1 administration (Fig. 4C, S14C, Supplementary movie 4). Thus, stem cells normally confine mitochondria containing old proteins to distinct sub-cellular domains by a Drp1-dependent mechanism, and such age-dependent localization of old mitochondria may be required for their asymmetric apportioning.

Our approaches for studying age-selective asymmetry during cell division show that mammalian epithelial stem-like cells allocate their mitochondria age-dependently and asymmetrically between daughters upon cell division. The mechanisms involved require normal functioning of the mitochondrial quality control machineries and mitochondrial fission that spatially restrict old mitochondrial matter to the perinuclear region of the mother cell. As our work was conducted on mammary epithelial stem-like cells *in vitro*, future work addressing the extent of the phenomenon in other stem cell compartments and *in vivo* is needed. Interestingly, asymmetric cell division of mammalian embryonic stem cells depends

on polarized paracrine signals (27) that could also further influence mitochondrial apportioning. Other recent evidence has implicated mitochondrial fitness in aging (4, 28, 29) and in tissue maintenance (30, 31). It will be important to determine whether the age-dependent asymmetric apportioning of mitochondria described here has a role in such physiologic processes.

Supplementary Material

Refer to Web version on PubMed Central for supplementary material.

Acknowledgements

REFERENCES

1. Rossi DJ, et al. Deficiencies in DNA damage repair limit the function of haematopoietic stem cells with age. Nature. 2007 Jun 7.447:725. [PubMed: 17554309]

2. Coumailleau F, Furthauer M, Knoblich JA, Gonzalez-Gaitan M. Directional Delta and Notch trafficking in Sara endosomes during asymmetric cell division. Nature. 2009 Apr 23.458:1051. [PubMed: 19295516]

3. Fichelson P, et al. Live-imaging of single stem cells within their niche reveals that a U3snoRNP component segregates asymmetrically and is required for self-renewal in Drosophila. Nature cell biology. 2009 Jun.11:685.

4. McFaline-Figueroa JR, et al. Mitochondrial quality control during inheritance is associated with lifespan and mother-daughter age asymmetry in budding yeast. Aging cell. 2011 Oct.10:885. [PubMed: 21726403]

5. Aguilaniu H, Gustafsson L, Rigoulet M, Nystrom T. Asymmetric inheritance of oxidatively damaged proteins during cytokinesis. Science. 2003 Mar 14.299:1751. [PubMed: 12610228]

6. Spokoini R, et al. Confinement to organelle-associated inclusion structures mediates asymmetric inheritance of aggregated protein in budding yeast. Cell reports. 2012 Oct 25.2:738. [PubMed: 23022486]

7. Rujano MA, et al. Polarised asymmetric inheritance of accumulated protein damage in higher eukaryotes. PLoS biology. 2006 Dec.4:e417. [PubMed: 17147470]

8. Hernebring M, et al. Removal of damaged proteins during ES cell fate specification requires the proteasome activator PA28. Sci Rep. 2013; 3:1381. [PubMed: 23459332]

9. Vilchez D, et al. Increased proteasome activity in human embryonic stem cells is regulated by PSMD11. Nature. 2012 Sep 13.489:304. [PubMed: 22972301]

10. Chaffer CL, et al. Normal and neoplastic nonstem cells can spontaneously convert to a stem-like state. Proceedings of the National Academy of Sciences of the United States of America. 2011 May 10.108:7950. [PubMed: 21498687]

11. Raouf A, et al. Transcriptome analysis of the normal human mammary cell commitment and differentiation process. Cell stem cell. 2008 Jul 3.3:109. [PubMed: 18593563]

12. Patterson GH, Lippincott-Schwartz J. A photoactivatable GFP for selective photolabeling of proteins and cells. Science. 2002 Sep 13.297:1873. [PubMed: 12228718]

13. Lee GM, Fong SS, Oh DJ, Francis K, Palsson BO. Characterization and efficacy of PKH26 as a probe to study the replication history of the human hematopoietic KG1a progenitor cell line. In Vitro Cell Dev Biol Anim. 2002 Feb.38:90. [PubMed: 11929001]

14. Keppler A, et al. A general method for the covalent labeling of fusion proteins with small molecules in vivo. Nature biotechnology. 2003 Jan.21:86.

15. Hernandez G, et al. MitoTimer: a novel tool for monitoring mitochondrial turnover. Autophagy. 2013 Nov 1.9:1852. [PubMed: 24128932]

16. Lukyanov KA, Chudakov DM, Lukyanov S, Verkhusha VV. Innovation: Photoactivatable fluorescent proteins. Nature reviews. Molecular cell biology. 2005 Nov.6:885.

17. Dontu G, et al. In vitro propagation and transcriptional profiling of human mammary stem/progenitor cells. Genes & development. 2003 May 15.17:1253. [PubMed: 12756227]

18. Okatsu K, et al. p62/SQSTM1 cooperates with Parkin for perinuclear clustering of depolarized mitochondria. Genes Cells. 2010 Aug.15:887. [PubMed: 20604804]

19. Mantel C, Messina-Graham S, Broxmeyer HE. Upregulation of nascent mitochondrial biogenesis in mouse hematopoietic stem cells parallels upregulation of CD34 and loss of pluripotency: a potential strategy for reducing oxidative risk in stem cells. Cell cycle. 2010 May 15.9:2008. [PubMed: 20495374]

20. Charruyer A, et al. CD133 is a marker for long-term repopulating murine epidermal stem cells. J Invest Dermatol. 2012 Nov.132:2522. [PubMed: 22763787]

21. Higuchi R, et al. Actin dynamics affect mitochondrial quality control and aging in budding yeast. Current biology : CB. 2013 Dec 2.23:2417. [PubMed: 24268413]

22. Lai CY, Jaruga E, Borghouts C, Jazwinski SM. A mutation in the ATP2 gene abrogates the age asymmetry between mother and daughter cells of the yeast Saccharomyces cerevisiae. Genetics. 2002 Sep.162:73. [PubMed: 12242224]

23. Smirnova E, Griparic L, Shurland DL, van der Bliek AM. Dynamin-related protein Drp1 is required for mitochondrial division in mammalian cells. Molecular biology of the cell. 2001 Aug. 12:2245. [PubMed: 11514614]

24. Vives-Bauza C, et al. PINK1-dependent recruitment of Parkin to mitochondria in mitophagy. Proceedings of the National Academy of Sciences of the United States of America. 2010 Jan 5.107:378. [PubMed: 19966284]

25. McLelland GL, Soubannier V, Chen CX, McBride HM, Fon EA. Parkin and PINK1 function in a vesicular trafficking pathway regulating mitochondrial quality control. The EMBO journal. 2014 Feb 18.33:282. [PubMed: 24446486]

26. Cassidy-Stone A, et al. Chemical inhibition of the mitochondrial division dynamin reveals its role in Bax/Bak-dependent mitochondrial outer membrane permeabilization. Developmental cell. 2008 Feb.14:193. [PubMed: 18267088]

27. Habib SJ, et al. A localized Wnt signal orients asymmetric stem cell division in vitro. Science. 2013 Mar 22.339:1445. [PubMed: 23520113]

28. Hughes AL, Gottschling DE. An early age increase in vacuolar pH limits mitochondrial function and lifespan in yeast. Nature. 2012 Dec 13.492:261. [PubMed: 23172144]

29. Rafelski SM, et al. Mitochondrial network size scaling in budding yeast. Science. 2012 Nov 9.338:822. [PubMed: 23139336]

30. Vazquez-Martin A, et al. Mitochondrial fusion by pharmacological manipulation impedes somatic cell reprogramming to pluripotency: new insight into the role of mitophagy in cell stemness. Aging. 2012 Jun.4:393. [PubMed: 22713507]

31. DuBoff B, Gotz J, Feany MB. Tau promotes neurodegeneration via DRP1 mislocalization in vivo. Neuron. 2012 Aug 23.75:618. [PubMed: 22920254]
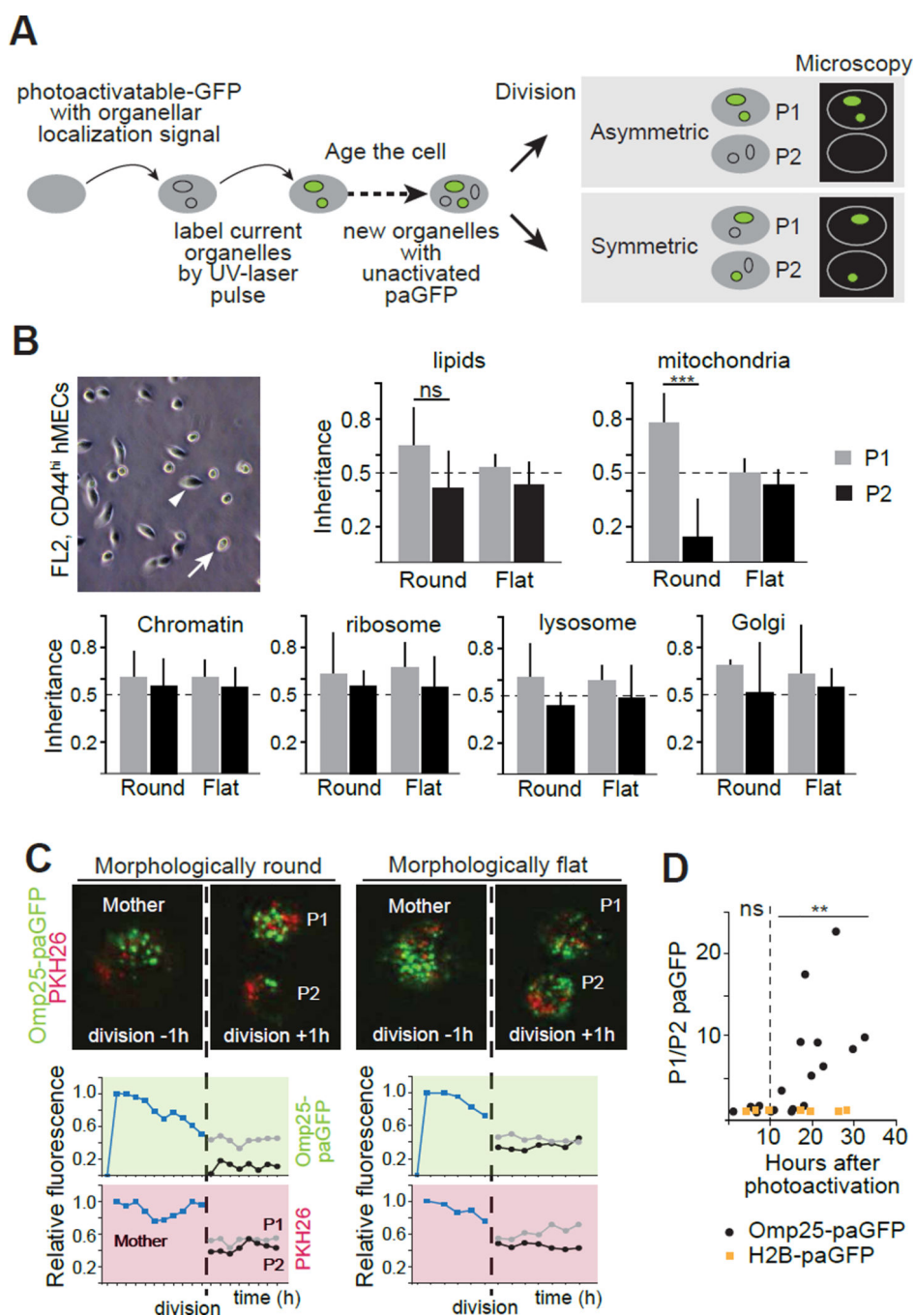
Fig. 1. Asymmetric apportioning of aged mitochondria during cell division
(**A**) Schematic of the labeling strategy using paGFP. (**B**) Analysis of apportioning of a fluorescent lipid dye, and of green fluorescence marking five paGFP-targeted organelles during cell division in epithelial (morphologically flat, arrowhead), and stem-like (morphologically round, arrow) cells in cultures of human mammary epithelium cells (hMECs). P1 and P2 indicate daughter cells, with P1 being the daughter receiving more of the targeted organelle. Inheritance indicates fluorescence of daughter cells relative to that of the mother cell scaled to 1. (**C**) Dynamics of mitochondrial apportioning in round SLCs and

flat epithelial cells. Representative divisions are shown with mitochondria in green (paGFP-Omp25) and the lipid dye (PKH26) in red. Images are frame captures from one hour before and after division, and fluorescence intensity per cell is plotted at one-hour intervals. (**D**) Analysis of asymmetric apportioning as a function of label age. SLCs dividing more than 10 hours after label activation show increasing asymmetric apportioning of mitochondria (Omp25), but not a chromatin label (H2B). Each data point represents an individual cell division. (**$p<0.01$, ***$p<0.001$, t-test)
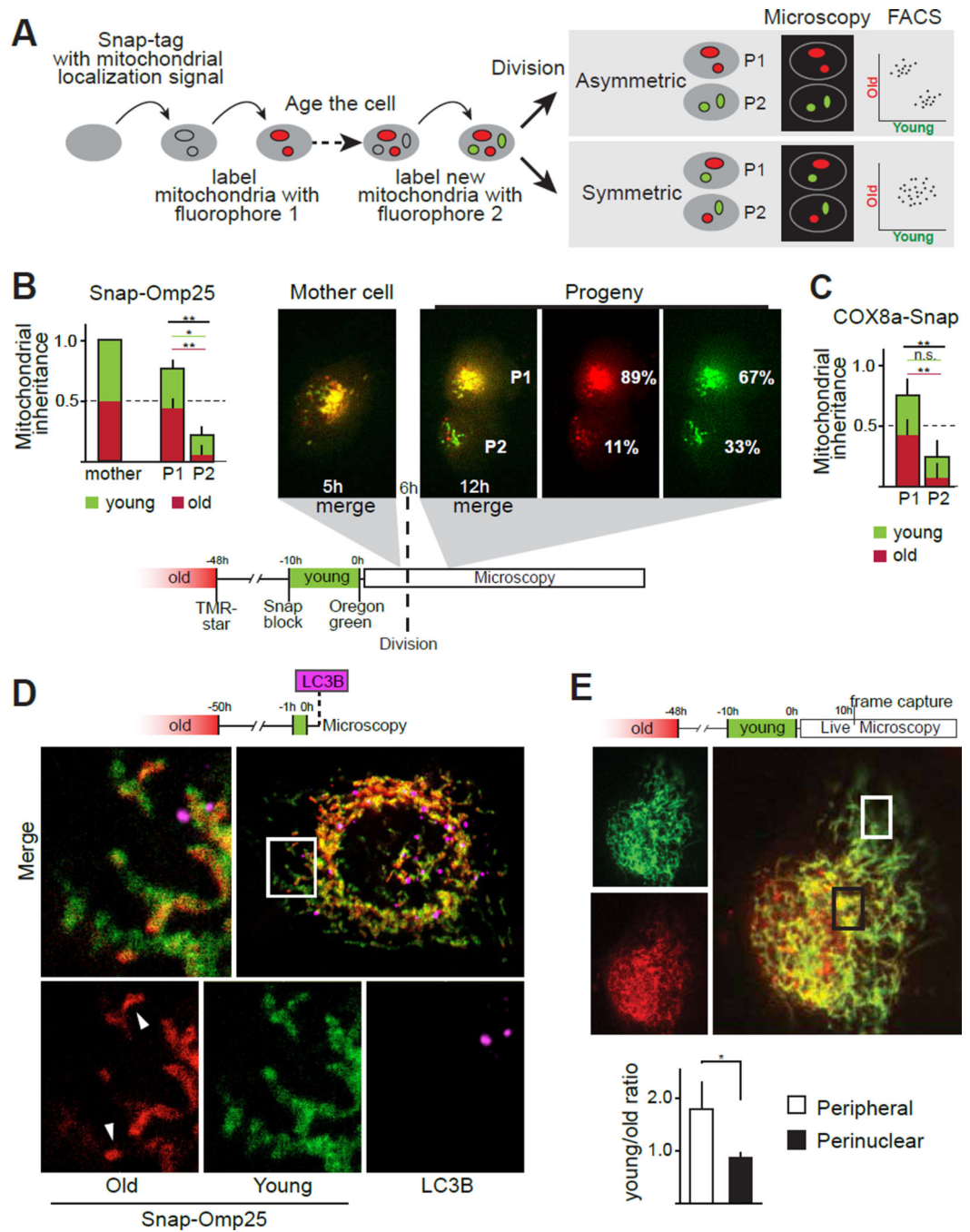
Fig. 2. Age-dependent segregation and subcellular localization of mitochondria
(**A**) Schematic of the labeling strategy using Snap-tag chemistry. (**B–C**) Analysis of mitochondrial outer membrane (B) and inner membrane (C) inheritance upon cell division. Red and green sections of bars represent the old and young labels, respectively. Values were scaled so that total intensity (red+green) of the mother cell is 1 (n=5). Representative division occurring at 6 hours after the second (green) label is shown. Percent values represent the average of five divisions. Original magnification 40×. (**D**) Confocal microscopy of a cell with 50 hour-old and 0 to 1 hour-old mitochondrial Snap-Omp25

labeled red and green, respectively. Mitochondrial network contains domains with different levels of enrichment for the old proteins. Mitochondrial domains enriched with old proteins (arrow heads) are not associated with autophagosomes detected by immunofluorescence for LC3B (purple) (63×, 2 μm Z-section). (**E**) Localization of old (red) and young (green) mitochondria (Snap-Omp25) 10 hours after labeling in an undivided cell. Squares mark regions used for measurements of the perinuclear and peripheral intensities in frames captured 10 hours after labeling for n=3 (cells imaged from three separate labeling experiments) (*p<0.05, **p<0.01, t-test).
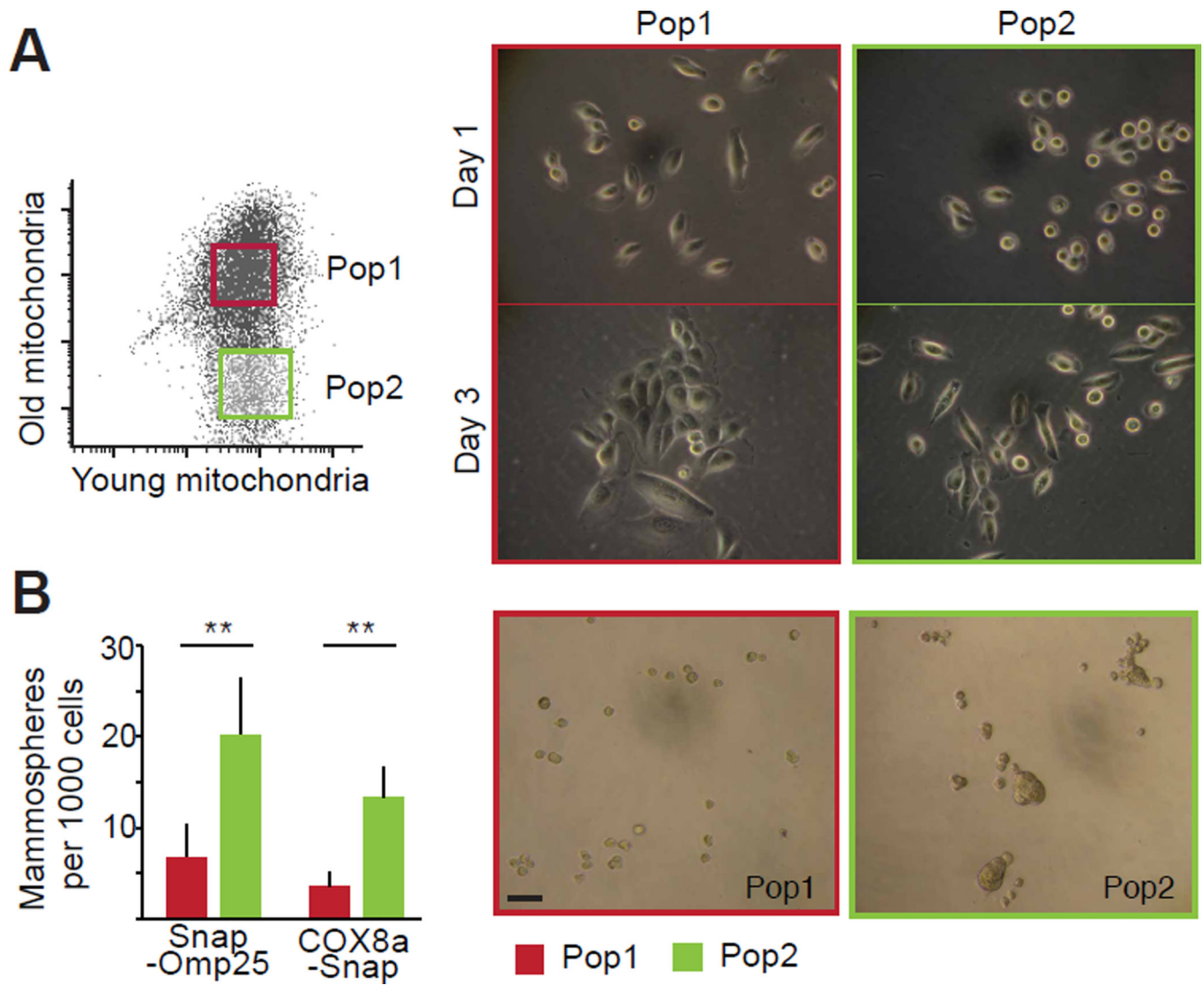
Fig. 3. Stemness properties of daughter cells receiving younger mitochondria
(**A**) FACS-mediated isolation of cell populations with high and low contents of old mitochondria (Pop1 and Pop2, respectively). Images show representative populations after 1 and 3 days in culture. (**B**) Mammosphere forming capacity of Pop1 and Pop2 cells for n=5 (scale bar 50μm, **p<0.01, t-test).
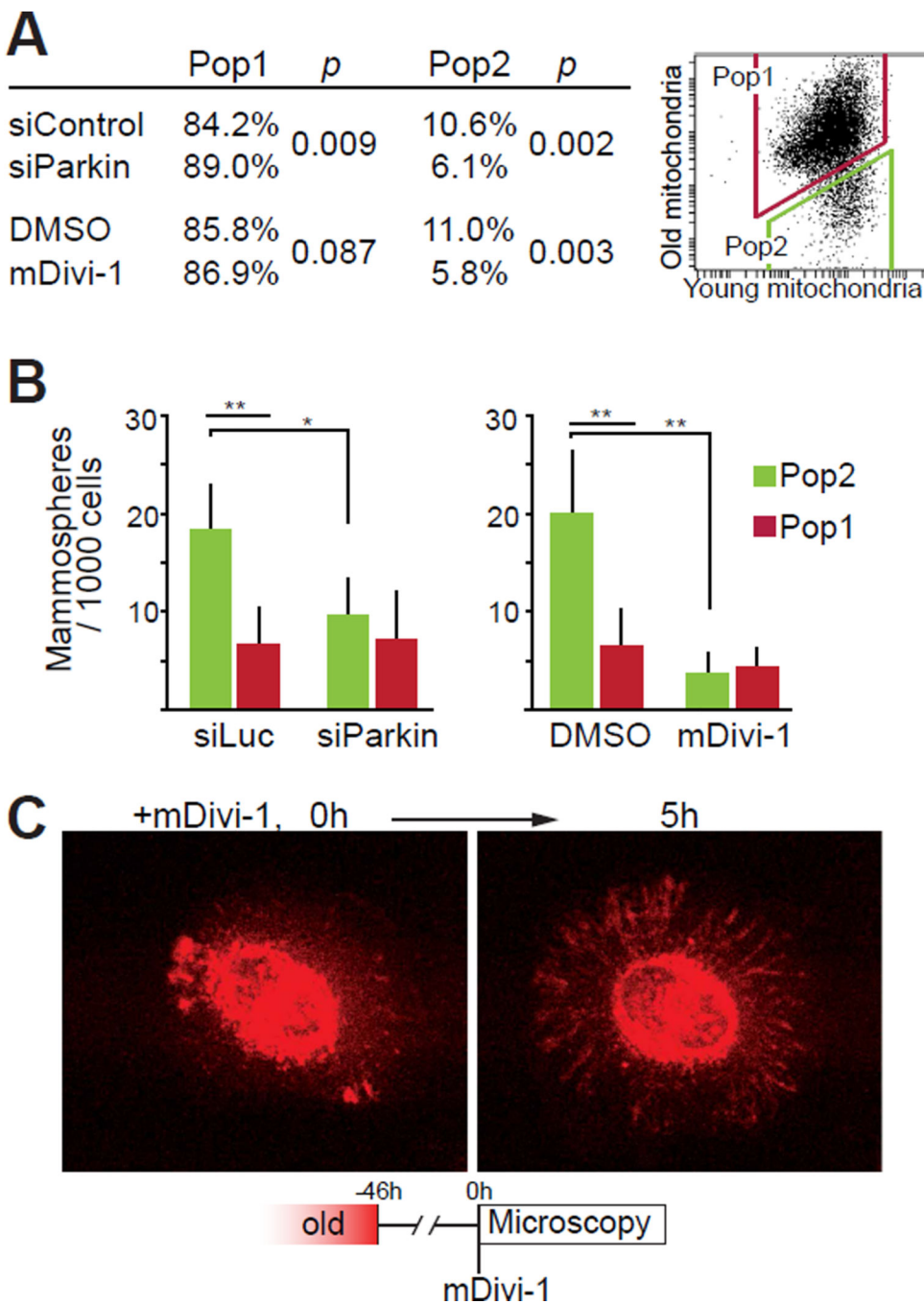
Fig. 4. Effects of mitochondrial quality control on asymmetric apportioning of old mitochondria during cell division

(**A**) FACS analyses of mitochondrial apportioning in cells with defective mitochondrial quality control induced by siRNA-mediated depletion of Parkin (siParkin) or pharmacological inhibition of mitochondrial fission (mDivi-1). Table presents the percentages of cells in the two populations for n=3. (**B**) Mammosphere-forming capacity of cells in Pop1 and Pop2 are equal following siRNA Parkin and mDivi-1 (n=3). (**C**) Localization of old mitochondria following treatment with mDivi-1. Images are frame

captures at start (0 hours) and 5 hours after mDivi-1 administration. Original magnification 63×. (*p<0.05, **p<0.01, t-test).